Simultaneous oxidation of alcohols and hydrogen evolution in a hybrid system under visible light irradiation

Fei Li[a,*], Yong Wang[a], Jian Du[a], Yong Zhu[a], Congying Xu[a], Licheng Sun[a,b]

[a] State Key Laboratory of Fine Chemicals, DUT-KTH Joint Education and Research Center on Molecular Devices, Dalian University of Technology, Dalian, 116024, China
[b] Department of Chemistry, School of Chemical Science and Engineering, KTH Royal Institute of Technology, 10044 Stockholm, Sweden

ARTICLE INFO

ABSTRACT

Water oxidation as a multi-electron transfer and endothermal reaction has been considered to be the bottleneck of solar-driven water splitting into oxygen and hydrogen. Herein, an alternative approach for solar energy conversion is developed by coupling H_2 generation with the selective oxidation of alcohol. In a closed redox system containing molecular ruthenium catalyst (RuCat) and Pt modified g-C_3N_4 (Pt-g-C_3N_4) composite, hydrogen production is concomitant with the oxidation of benzyl alcohols to aldehydes with over 99% selectivity in the presence of visible light and pure water. By contrary, the system lacking molecular catalyst only exhibits low to moderate selectivities towards aldehydes. The remarkably improved selectivity is attributed to the formation of highly active Ru(IV) = O intermediate through efficient hole transfer from g-C_3N_4 to RuCat.

1. Introduction

Photocatalytic water splitting into hydrogen and oxygen is a promising approach for solar energy conversion [1,2]. Powdered system based on semiconductors is the simplest water-splitting system that is more amenable to cheap, large-scale production of H_2 [3–8]. Nevertheless, the oxidation of water severely restricts the efficiency of overall water splitting due to its sluggish kinetics and endergonic thermodynamics [9,10]. Furthermore, the product of water oxidation, O_2, is not of significant value and always detrimental to the hydrogen evolution reaction [11]. Besides water splitting, an overlooked approach for solar energy conversion is producing H_2 from alternative sources such as abundant biomass [12,13]. These reactions are generally easier in kinetics ($2e^-/2H^+$ coupled process), require less activation energy and yield easily separated and high-value products [14]. Among them, selective oxidation of benzyl alcohols to aldehydes by visible light is of great significance in both laboratorial and industrial scale [15–17]. At present, classical aldehydes production reactions are still employed in the presence of organic solvents, hazardous oxidants and high pressure/temperature [11]. Therefore, a green synthetic route is urgently necessary. Inspired by various types of enzymes in the organism, which are capable to perform highly selective and efficient oxidation of organic molecules, transition-metal complexes are considered as good candidates to catalyze selective oxidation of benzyl alcohols. As a result, significant progresses have been made in constructing molecular catalysts based system with [Ru(bpy)$_3$]$^{2+}$ (bpy = 2,2'-bipyridine) as

the photosensitizer [18–21]. However, the narrow absorption spectrum, easily photo-induced decomposition and expensive features of ruthenium make [Ru(bpy)$_3$]$^{2+}$ almost impossible towards large scale application. Instead, semiconductors possess the characteristics of wide and continuous absorption spectrum, outstanding stability and popular price. So incorporation of the efficient transition-metal complexes with photoactive semiconductors is an ideal approach. To date, little research effort has been made based on this concept and most of them are performed in the presence of sacrificial reagent [22,23], which impedes the sustainable way of converting solar energy into chemical fuels. Moreover, the utilization of organic solvent and acidic solution are not environmentally benign [24]. Therefore, a high-selective and stable photocatalytic system able to simultaneously oxidize benzyl alcohols and produce H_2 in pure water is preferable.

As a proof-or-concept, we present here the combination of a ruthenium molecular catalyst and platinum particle modified graphitic carbon nitride (Pt-g-C_3N_4) for selective oxidation of benzyl alcohols coupled with H_2 evolution in pure water under visible light irradiation. The experimental results reveal that the introduction of Ru catalyst plays an essential role in improving the selectivity of benzyl alcohols oxidation in this hybrid system.

---

* Corresponding author.
  E-mail address: lifei@dlut.edu.cn (F. Li).

2. Experimental

2.1. Materials and methods

All reactions were carried out under an argon atmosphere. Organic substrates such as benzyl alcohol, 4-methoxybenzyl alcohol, 4-methyl-benzyl alcohol, 4-chlorobenzyl alcohol, cinnamyl alcohol and cyclo-hexanol as well as the corresponding aldehydes were purchased from Aladdin Industrial Corporation and used without further purification. Ultra-pure water (18.2 MΩ cm^{-1}) for all the reactions was obtained from a Milli-Q system (Millipore, Direct-Q 3 UV). All other chemicals are commercially available.

SEM micrographs were obtained by using a Nova NanoSEM 450 instrument. TEM images were conducted with FEI TF30 equipment. X-ray diffraction was collected with a D/max-2400 diffractometer. UV–vis diffuse reflectance spectra measurement was performed on an Evolution 200 spectrophotometer (Thermo, USA). Fourier transform infrared (FTIR) spectra were recorded on a Thermo Fisher 6700 spectrometer, and the samples were prepared as KBr tablets. ^{1}H NMR spectrum was recorded at 298 K using a Bruker DRX-400 instrument operating at 400 MHz. UV–vis absorption measurement was taken with an Agilent 8453 spectrophotometer. Steady-state and time resolved photoluminescence (PL) measurements were performed by use of nanosecond flash-photolysis system (LP920, Edinburgh Instruments).

2.2. Preparation of Pt-g-C₃N₄

g-C₃N₄ was prepared according to the protocol reported in literature [25]. In brief, a set amount of precursor (urea, dicyandiamide (DCDA), thiourea and cyanamide) was put in a lidded high quality alumina crucible, then placed inside a muffle furnace and heated with a heating rate of 2 °C/min, and finally held at the target temperature 530 °C for 2 h in the air flow. The resultant powders were used directly without other treatment. Pt cocatalyst was deposited onto g-C₃N₄ using a photodeposition method. Stock solutions of ultra-pure water and H₂PtCl₆·6H₂O were made beforehand and then added according to the required weight of metal (1 wt% was found to be the optimal loading for Pt). Photodeposition reaction was performed in 100 mL water:-methanol (9:1, v/v) solution containing 100 mg g-C₃N₄ and certain amount of Pt, the reactor was sealed and purged with Ar gas for 30 min, then irradiated for 1 h under full arc irradiation using a 300 W Xe lamp. The photocatalyst was then filtered and washed three times with water, finally dried at 70 °C under vacuum for overnight.

2.3. Synthesis of [Ru(tpa)(H₂O)₂](PF₆)₂

This complex was synthesized according to the literature's method with some modification. Briefly, to a refluxed solution of RuCl₃·3H₂O (0.20 g, 0.764 mmol) in ethanol (30 mL) was added TPA ligand (0.222 g, 0.764 mmol). After refluxing for 10 min, 20 mL of an aqueous solution of AgNO₃ (0.39 g, 2.294 mmol) was added. The mixture was then refluxed for 24 h, and the precipitate was removed by filtration. Then a small amount of saturated NH₄PF₆ solution was added to the filtrate dropwise and the precipitate was collected by filtration. After washing with ether and drying under vacuum, a dark green solid was obtained. Yield: 0.2 g (35%). ^{1}H NMR (400 MHz, CD₃CN): δ 4.25 (s, 2H), 4.70 and 4.99 (ABq, 4H), 6.82 (d, 1H), 6.87 (t, 2H), 6.97 (t, 1H), 7.33 (t, 1H), 7.43 (d, 2H), 7.67 (t, 2H), 8.41 (d, 2H), 8.80 (d, 1H).

2.4. Photocatalytic experiments

Photocatalytic dehydrogenation reactions were performed in a 50 mL Schlenk bottle with 10 mL pure water containing 10 mg Pt-g-C₃N₄ photocatalyst, 0.08 mM RuCat and 10 mM corresponding alcohols. The reactor was sealed, degassed with Ar gas for 30 min and then irradiated by a 300 W Xe lamp equipped with a cutoff filter

(λ > 400 nm). The temperature of the reaction system was maintained by a custom-built jacketed cooler. The generated H₂ in the headspace was analyzed and quantified by gas chromatography (Techcomp GC 7890T, Ar carrier gas, Thermo Conductivity Detector). When reaction finished, the resultant solution was centrifuged and the supernatant was extracted with 3 × 10 mL CH₂Cl₂ and dried with anhydrous Na₂SO₄. Then the solvent was removed by rotary evaporation to ca. 3 mL, the product was analyzed and quantified by gas chromatography (Agilent GC 6890N, N₂ carrier gas, Flame Ionization Detector). Dodecane was selected as the internal standard to quantify the converted alcohols and generated aldehydes. In addition, ^{1}H NMR spectroscopy was also adopted for characterizing and quantifying the organic products. The conversion and selectivity efficiency was calculated according to Eqs. (1) and (2):

$$Conversion(\%) = \frac{n_{initial\ alcohol} - n_{residual\ alcohol}}{n_{initial\ alcohol}} \times 100\% \tag{1}$$

$$Selectivity(\%) = \frac{n_{produced\ aldehyde}}{n_{initial\ alcohol} - n_{residual\ alcohol}} \times 100\% \tag{2}$$

Apparent quantum yield (AQY) was defined as the ratio between the number of collected carriers and the number of all the incident photons on the device active area at a given wavelength. It could be calculated according to the following equation:

$$AQY\% = \frac{2n_{H_2} \cdot N_A \cdot h \cdot c}{I \cdot \lambda \cdot A \cdot t} \cdot 100 \tag{3}$$

Where n_{H2} is the moles of photogenerated H₂, N_A is Avogadro's constant (6.02 × 10²³ mol^{-1}), h is the Planck constant (6.63 × 10^{-34} J s), c is the speed of light (3 × 10⁸ m s^{-1}), I is the light intensity, λ is the wavelength of incident monochromatic light, A is the cross-sectional area of irradiation and t is the irradiation time.

3. Results and discussion

3.1. Photocatalytic performance of Pt-g-C₃N₄ composite

The discovery of g-C₃N₄ as a metal-free photocatalyst by Wang et al. has stimulated intensive research in the application this two-dimensional conjugated polymer [26–31]. g-C₃N₄ has suitable valence and conduction band positions for either water splitting or CO₂ reduction [3,25,32–34]. In addition, the g-C₃N₄-based materials have also been found to act as photocatalysts for organic redox synthesis [35–37]. The well positioned band edges make it the best candidate for coupling benzyl alcohols oxidation with proton reduction.

At the beginning of our research, Pt doped g-C₃N₄ (Pt-g-C₃N₄) was used as the photocatalyst for 4-methoxybenzyl alcohol (MBA) oxidation. Photocatalytic reactions were carried out in 10 mL water containing Pt-g-C₃N₄ (10 mg) and MBA (0.1 mmol), the light source was a 300 W Xe lamp equipped with a 400 nm cut-off filter. The g-C₃N₄ was prepared with different precursors (urea, dicyandiamide (DCDA), thiourea and melamine) according to the reported protocols [25], in which urea derived g-C₃N₄ exhibited the best activity towards alcohols dehydrogenation (Fig. S3). The scanning electron microscopy (SEM) and transmission electron microscopy (TEM) images, powdered X-ray diffraction (XRD) pattern and UV–vis diffuse reflectance (DRS) spectrum of urea based g-C₃N₄ agreed well with the literature's data (Figs. , S1 and S2). As shown in Fig. S4a, the H₂ and 4-methoxybenzyl aldehyde (MBAd) yields increased with the loading of Pt up to 1 wt%, more Pt loading resulted in the decreased activity probably due to the aggregation of Pt which reduces light absorption. On the contrary, preliminary kinetic investigations suggest that the reaction rate is almost zero order with respect to the amount of Pt-g-C₃N₄, so 10 mg of Pt-g-C₃N₄ was used in photocatalysis to run the reaction in a relatively well-dispersed solution (Fig. S4b).

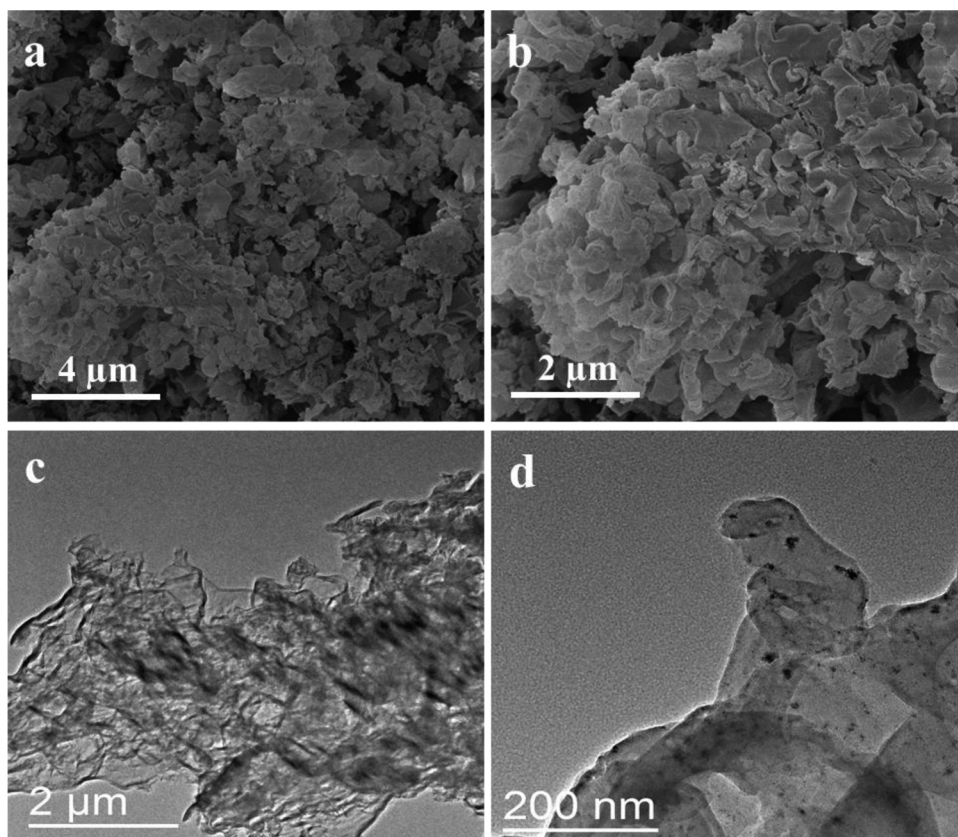The results of photocatalytic dehydrogenation with different

Fig. 1. (a,b) SEM images of g-C_3N_4 synthesized from urea. (c) TEM image of urea derived g-C_3N_4. (d) TEM micrograph of Pt-g-C_3N_4 composite.

Table 1
Dehydrogenation of primary aromatic alcohols using Pt-g-C_3N_4 as a photocatalyst.[a]

Entry	Substrate	Product	Conv.[%]	Sel.[%]	H_2[μmol]
1			40	90	51
2			97	51	125
3			> 99	67	132
4			> 99	56	130
5			55	61	79
6			37	78	45

[a] Reaction conditions: Ar atmosphere, 10 mg Pt-g-C_3N_4 powder and 10 mM alcohols in 10 mL pure water without any pH adjustment were irradiated with a 300 W Xe lamp equipped with a 400 nm cut-off filter at room temperature for 20 h.

Fig. 2. Time-dependent photocatalytic dehydrogenation of MBA by Pt-g-C_3N_4. Conversion, selectivity (towards aldehyde), and carbon balance are scaled on the right axis, while the amounts of products are scaled on the left axis.

alcohols are summarized in Table 1. Compared with the unsubstituted benzyl alcohol (BA), alcohols bearing both electron-donating and electron-withdrawing functional groups exhibited better conversion and H_2 yields (Table 1, Entries 2–4), but the selectivities for aldehydes were unsatisfactory. Especially for MBA, only 51% selectivity was obtained after irradiation for 20 h (Table 1, Entry 2). In addition, the oxidation of other alcohols such as chnnamyl alcohol and cyclohexanol were also available in the current system (Table 1, Entries 5–6). Both of them were able to be transformed into the corresponding aldehydes together with H_2 evolution smoothly. Likewise, only moderate selectivity was obtained. To gain more information about the poor selectivity, the reaction of MBA dehydrogenation was monitored for a reaction period of 20 h, with a detailed analysis of reaction intermediates/products and the carbon balance (Fig. 2). This investigation shows the selectivity of MBAd was declining across the entire reaction period. The over-oxidation of MBA to 4-methoxy-benzoic acid and CO_2
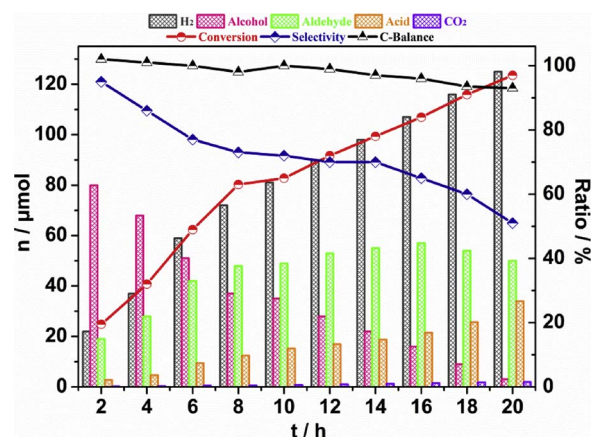
occurred and the amounts of byproducts increased with the reaction time. Carbon balance shows that there is no other byproduct generated during the reaction period. Based on these results, the poor selectivity for aldehyde is due to the strong oxidative nature of photogenerated holes.

3.2. Feasibility study of combining g-C_3N_4 photocatalyst and RuCat

To improve the selectivity of benzyl alcohols' oxidation, a molecular catalyst [Ru(tpa)(H_2O)$_2$]$^{2+}$ (RuCat, tpa = tris(2-pyridylmethyl)amine) that is well-studied in catalytic conversion of alcohol to aldehyde was chosen to incorporate with Pt-g-C_3N_4 [19,22,38]. By comparing the redox potentials of g-C_3N_4 and RuCat (Fig. 3a), photo-generated holes were anticipated to transfer from g-C_3N_4 to RuCat and produce Ru(IV)
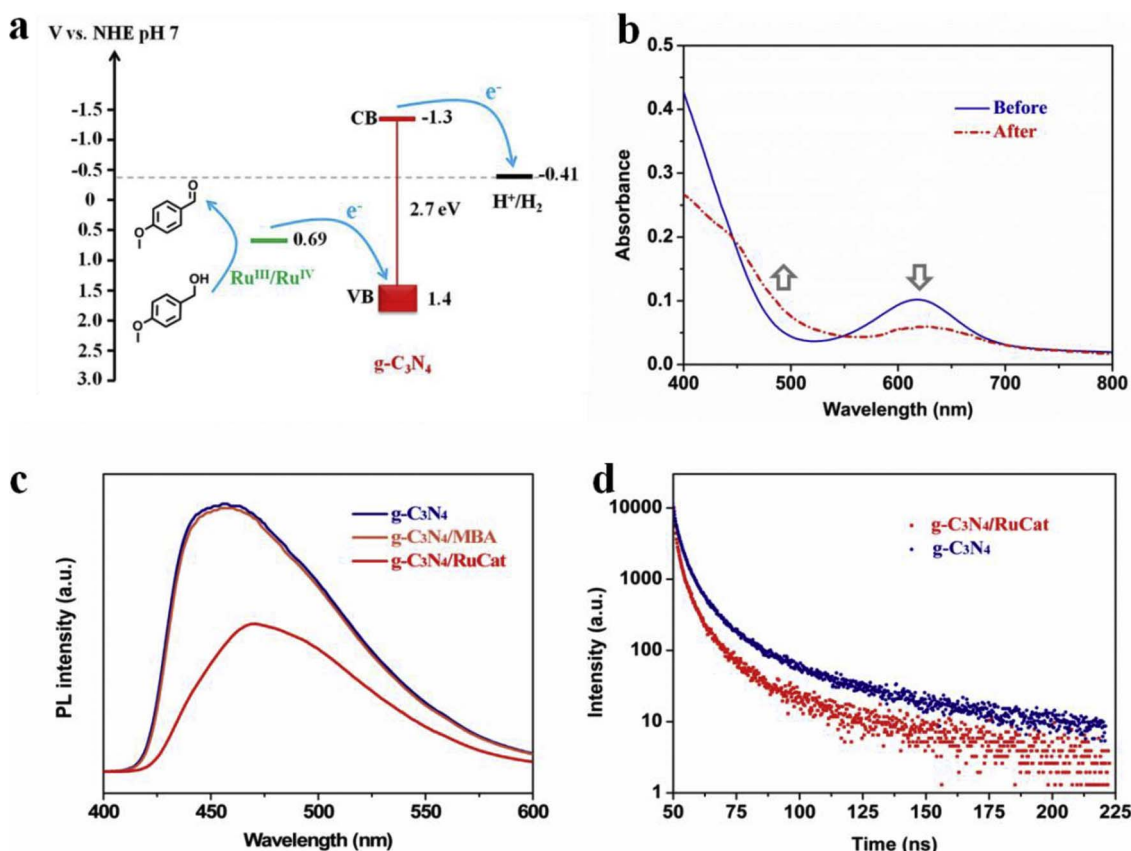
Fig. 3. (a) Energy level diagram of g-C$_3$N$_4$, RuCat and H$_2$ production. (b) UV–vis absorption spectra of 0.08 mM of RuCat in 10 mL pure water containing 15 mg Pt-g-C$_3$N$_4$ before (blue) and after (red) light irradiation for 10 min (Pt-g-C$_3$N$_4$ powder was removed by filter membrane). (c) Photoluminescence spectra of g-C$_3$N$_4$ (blue), g-C$_3$N$_4$/MBA (orange) and g-C$_3$N$_4$/RuCat (red) excited at a wavelength of 400 nm. (d) Time-resolved photoluminescence spectra under 400 nm excitation at 298 K for g-C$_3$N$_4$ (blue) and g-C$_3$N$_4$/RuCat (red). (For interpretation of the references to colour in this figure legend, the reader is referred to the web version of this article.)

= O intermediate, which is highly active for the selective oxidation of alcohol. The formation of the high-valent Ru(IV) = O species was evidenced by UV–vis spectroscopy. In detail, a reaction sample containing RuCat and Pt-g-C$_3$N$_4$ was irradiated for 10 min, g-C$_3$N$_4$ was removed and the UV–vis absorption spectrum of the resulting solution was recorded. As shown in Fig. 3b, the band at 620 nm greatly decreases and a new absorption band (shoulder) at 470 nm appears. According to our previous study, this new absorption band was ascribed to the formation of Ru(IV) = O species [22]. To gain more insights into the charge transfer process between g-C$_3$N$_4$ and RuCat, steady state photoluminescence (PL) experiment was performed. Excited at 340 nm, the luminescence of g-C$_3$N$_4$ was largely quenched upon the addition of RuCat, indicating that charge transfer between g-C$_3$N$_4$ and RuCat could greatly suppress the radiative electron-hole recombination (Fig. 3c). On the contrary, the emission of g-C$_3$N$_4$ was almost unaffected upon adding MBA. In addition, the charge transfer process was investigated by time-resolved photoluminescence (TRPL). As shown in Fig. 3d of the fitting results, the average lifetime of g-C$_3$N$_4$ and RuCat/g-C$_3$N$_4$ samples is 1.8 and 0.39 ns, respectively. Clearly, RuCat/g-C$_3$N$_4$ mixture has much shorter PL lifetimes and better electron migration capacity, which was believed to highly facilitate photocatalytic reaction.

3.3. Photocatalytic performance of Pt-g-C$_3$N$_4$/RuCat hybrid system

Having confirmed the formation of Ru(IV) = O and efficient charge transfer between RuCat and g-C$_3$N$_4$, the performance of photocatalytic oxidation of MBA by RuCat/Pt-g-C$_3$N$_4$ was evaluated. After irradiated under continuous stirring for 10 h, MBAd was almost exclusively generated and hydrogen was simultaneously produced without any oxygen evolution (Table 2, entry 7). Gas chromatography and ^{1}H NMR spectra

Table 2
Photocatlytic conversion of MBA to MBAd and H$_2$.[a]

Entry	Cat.	T[h]	Conv.[%]	Sel.[%]	H$_2$[μmol]	TON[d]
1[b]	RuCat/Pt-g-C$_3$N$_4$	10	trace	–	n.d.	–
2	–	10	–	–	n.d.	–
3	g-C$_3$N$_4$	10	–	–	n.d.	–
4	RuCat	10	trace	–	n.d.	–
5	RuCat/g-C$_3$N$_4$	10	9	> 99	9	21
6	Pt-g-C$_3$N$_4$	10	65	66	81	–
7	RuCat/Pt-g-C$_3$N$_4$	10	46	> 99	45	107
8	RuCat/Pt-g-C$_3$N$_4$	20	68	91	74	144
9	Pt-g-C$_3$N$_4$	20	97	51	125	–
10[c]	RuCat/Pt-g-C$_3$N$_4$	10	47	85	56	178

[a] Reaction conditions: 10 mg Pt-g-C$_3$N$_4$ powder, 0.08 mM RuCat and 10 mM MBA in 10 mL pure water without any pH adjustment were irradiated with a 300 W Xe lamp equipped with a 400 nm cut-off filter at room temperature.
[b] Dark conditions.
[c] 0.04 mM RuCat was used.
[d] TON = the mol of MBAd produced/the mol of RuCat adsorbed on the surface of Pt-g-C$_3$N$_4$.

showed essentially no acid or CO$_2$ generation (Fig. S6). Control experiments confirmed that no MBAd or H$_2$ could be detected in the absence of Pt-g-C$_3$N$_4$, light or loaded Pt, indicating each component is indispensible for efficient photocatalysis (Table 2, entry 1–4). However, the RuCat free system only attained 66% selectivity in the same reaction period (Table 2, entry 6). The adsorption of RuCat on Pt-g-C$_3$N$_4$ could be well described by the Freundlich equation (Fig. S5), indicating 54% of Ru complex was adsorbed under equilibrium condition, which is far exceeding the amount based on normal physical adsorption. This was considered as a result of the electrostatic interaction between
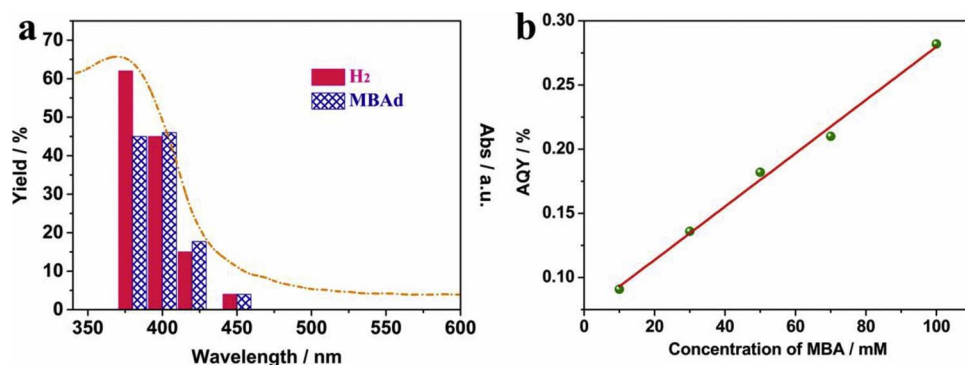
positively charged RuCat and Pt-g-C$_3$N$_4$ whose surface are negative charged. Evidently, the negatively charged surface of carbon nitride was supported by a Zeta potential of -21.7 mV under the reaction conditions. Based on the amount of absorbed RuCat, a turnover number (TON) of 107 was obtained for MBAd production. This value is almost 4-fold larger than that of a previous system using molecular photosensitizers [39]. However, the lack of Pt particles only attained 9% conversion efficiency, which demonstrated the significance of Pt loading in enhancing the activity of photocatalytic reaction (Table 2, entry 5). By extending the reaction period from 10 to 20 h, a higher conversion with a TON of 144 was obtained with a slightly decreased selectivity (91%, Table 2, entry 8), which might be ascribed to the partial decomposition of molecular catalyst during long-term irradiation. In agreement with this assumption, a decreased selectivity was observed by reducing the concentration of RuCat to half (Table 2, entry 10). It is notable that the selectivities achieved in the presence of RuCat were far better than that of RuCat free system (51%, Table 2, entry 9), highlighting the essential role of molecular catalyst on selectivity improvement. However, the reaction rate of alcohol dehydrogenation in the hybrid system was not as fast as that of molecular catalyst free system, which might be ascribed to different pathways for alcohol oxidation mediated by either high-valent Ru(IV) = O or photogenerated holes.

With MBA as the substrate, the yields of MBAd and H$_2$ exhibited linear increase with the illumination period, however, kept constant when the light was off (Fig. S7), confirming that the generation of MBAd and H$_2$ was due to the photoinduced MBA oxidation. The dependence of this hybrid system on the wavelength of incident light was also investigated. As depicted in Fig. 4a, the tendency of H$_2$ production corresponds well with the absorbance spectrum of g-C$_3$N$_4$ photocatalyst. Meanwhile, the selectivity of MBAd generation is reduced when the reaction performed at wavelength less than 400 nm. This illustrates the importance of visible light rather than UV light towards selective chemical conversion. The apparent quantum yield (AQY) of RuCat/Pt-g-C$_3$N$_4$ system was tested at 400 nm with different concentrations of MBA. As shown in Fig. 4b, the AQY based on MBAd exhibits first order with respect to the concentration of MBA and reaches 0.28% when 0.1 M substrate used. The stability test showed that the Pt-g-C$_3$N$_4$ composite can be re-used without apparent loss in both conversion and selectivity for at least five consecutive runs (Fig. S8). This can, in principle, be explained by the robust chemical inertness and the excellent stability of g-C$_3$N$_4$ towards photocorrosion. In addition, XRD, FTIR and SEM analyses of used Pt-g-C$_3$N$_4$ photocatalyst showed no obvious change after five reaction cycles (Figs. S9 and S10).

Encouraged by these results, photocatalytic reactions were extended to other aromatic alcohols. As shown in Table S1, all substrates were selectively transformed with the selectivity for aldehyde significantly higher (>90%) than that of RuCat free system. Specifically, the unsaturated carbon-carbon bonds of cinnamyl alcohol were well maintained during the photocatalytic generation of aldehyde (Table S1, entry 4).

4. Conclusions

In summary, we present here a hybrid photocatalytic system containing a molecular catalyst and Pt particle modified g-C$_3$N$_4$ for simultaneous oxidation of benzyl alcohols and production of H$_2$. It is remarkable that the incorporation of RuCat dramatically improves the selectivity towards aldehydes production due to the formation of highly active Ru(IV) = O intermediate. UV–vis and PL spectroscopy evidenced that the photogenerated holes are transfered from carbon nitride to molecular catalyst rather than the substrate, thus initiates metal-based selective oxidation. These findings bridge the gap between homogeneous and heterogeneous photocatalysis towards organic synthesis that utilize sunlight energy. The advantage of molecular catalyst in directly tuning the selectivity of photocatalytic organic transformation in a semiconductor-molecular hybrid system is promising, which has not been reported in previous studies. Attempt to extend the current system to other organic transformation reactions is now underway in our laboratory.

Appendix A. Supplementary data

Supplementary data associated with this article can be found, in the online version, at https://doi.org/10.1016/j.apcatb.2017.11.072.

References

[1] N.S. Lewis, D.G. Nocera, Proc. Natl. Acad. Sci. U. S. A. 103 (2006) 15729–15735.
[2] N.S. Lewis, Science 351 (2016) aad1920.
[3] J. Liu, Y. Liu, N. Liu, Y. Han, X. Zhang, H. Huang, Y. Lifshitz, S.-T. Lee, J. Zhong, Z. Kang, Science 347 (2015) 970–974.
[4] Q. Wang, T. Hisatomi, Q. Jia, H. Tokudome, M. Zhong, C. Wang, Z. Pan, T. Takata, M. Nakabayashi, N. Shibata, Y. Li, I.D. Sharp, A. Kudo, T. Yamada, K. Domen, Nat. Mater. 15 (2016) 611–615.
[5] J. Chen, D. Zhao, Z. Diao, M. Wang, S. Shen, Sci. Bull. 61 (2016) 292–301.
[6] H. Yu, R. Shi, Y. Zhao, T. Bian, Y. Zhao, C. Zhou, G.I.N. Waterhouse, L.-Z. Wu, C.-H. Tung, T. Zhang, Adv. Mater. 29 (2017) 1605148.
[7] R. Shi, Y. Cao, Y. Bao, Y. Zhao, G.I. Waterhouse, Z. Fang, L.-Z. Wu, C.-H. Tung, Y. Yin, T. Zhang, Adv. Mater. 29 (2017) 1700803.
[8] N. Tian, Y. Zhang, X. Li, K. Xiao, X. Du, F. Dong, G.I.N. Waterhouse, T. Zhang, H. Huang, Nano Energy 38 (2017) 72–81.
[9] J.J. Concepcion, J.W. Jurss, M.K. Brennaman, P.G. Hoertz, A.O.T. Patrocinio, N.Y. Murakami Iha, J.L. Templeton, T.J. Meyer, Acc. Chem. Res. 42 (2009) 1954–1965.
[10] P. Du, R. Eisenberg, Energy Environ. Sci. 5 (2012) 6012–6021.
[11] H. Kasap, C.A. Caputo, B.C.M. Martindale, R. Godin, V.W.-h. Lau, B.V. Lotsch, J.R. Durrant, E. Reisner, J. Am. Chem. Soc. 138 (2016) 9183–9192.
[12] R.M. Navarro, M.C. Sánchez-Sánchez, M.C. Alvarez-Galvan, F. del Valle, J.L.G. Fierro, Energy Environ. Sci. 2 (2009) 35–54.
[13] H.G. Cha, K.-S. Choi, Nat. Chem. 7 (2015) 328–333.

[14] T.P.A. Ruberu, N.C. Nelson, I.I. Slowing, J. Vela, J. Phys. Chem. Lett. 3 (2012) 2798–2802.
[15] P. Barbaro, C. Bianchini, Wiley-VCH, Weinheim, (2009) 393–438.
[16] R.J. Angelici, ACS Catal. 1 (2011) 772–776.
[17] W. Song, A.K. Vannucci, B.H. Farnum, A.M. Lapides, M.K. Brennaman, B. Kalanyan, L. Alibabaei, J.J. Concepcion, M.D. Losego, G.N. Parsons, T.J. Meyer, J. Am. Chem. Soc. 136 (2014) 9773–9779.
[18] F. Li, M. Yu, Y. Jiang, F. Huang, Y. Li, B. Zhang, L. Sun, Chem. Commun. 47 (2011) 8949–8951.
[19] D. Kalita, B. Radaram, B. Brooks, P.P. Kannam, X. Zhao, ChemCatChem 3 (2011) 571–573.
[20] X. Wu, X. Yang, Y.-M. Lee, W. Nam, L. Sun, Chem. Commun. 51 (2015) 4013–4016.
[21] S. Fukuzumi, T. Kishi, H. Kotani, Y.-M. Lee, W. Nam, Nat. Chem. 3 (2011) 38–41.
[22] X. Zhou, F. Li, X. Li, H. Li, Y. Wang, L. Sun, Dalton Trans. 44 (2015) 475–479.
[23] L. Bai, F. Li, Y. Wang, H. Li, X. Jiang, L. Sun, Chem. Commun. 52 (2016) 9711–9714.
[24] Z. Liu, J. Caner, A. Kudo, H. Naka, S. Saito, J. Chem Eur. 19 (2013) 9452–9456.
[25] D.J. Martin, K. Qiu, S.A. Shevlin, A.D. Handoko, X. Chen, Z. Guo, J. Tang, Angew. Chem. Int. Ed. 53 (2014) 9240–9245.
[26] X. Wang, K. Maeda, A. Thomas, K. Takanabe, G. Xin, J.M. Carlsson, K. Domen, M. Antonietti, Nat. Mater. 8 (2009) 76–80.
[27] X. Wang, X. Chen, A. Thomas, X. Fu, M. Antonietti, Adv. Mater. 21 (2009)

[28] J. Sun, J. Zhang, M. Zhang, M. Antonietti, X. Fu, X. Wang, Nat. Commun. 3 (2012) 1139.
[29] J. Zhang, G. Zhang, X. Chen, S. Lin, L. Möhlmann, G. Dołęga, G. Lipner, M. Antonietti, S. Blechert, X. Wang, Angew. Chem. Int. Ed. 51 (2012) 3183.
[30] J. Zhang, M. Zhang, R.Q. Sun, X. Wang, Angew. Chem. Int. Ed. 51 (2012) 10145–10149.
[31] J. Zhang, M. Zhang, L. Lin, X. Wang, Angew. Chem. Int. Ed. 54 (2015) 6297.
[32] G. Zhang, Z.-A. Lan, L. Lin, S. Lin, X. Wang, Chem. Sci. 7 (2016) 3062–3066.
[33] R. Kuriki, K. Sekizawa, O. Ishitani, K. Maeda, Angew. Chem. Int. Ed. 54 (2015) 2406–2409.
[34] R. Kuriki, H. Matsunaga, T. Nakashima, K. Wada, A. Yamakata, O. Ishitani, K. Maeda, J. Am. Chem. Soc. 138 (2016) 5159–5170.
[35] F. Su, S.C. Mathew, G. Lipner, X. Fu, M. Antonietti, S. Blechert, X. Wang, J. Am. Chem. Soc. 132 (2010) 16299–16301.
[36] Y. Chen, J. Zhang, M. Zhang, X. Wang, Chem. Sci. 4 (2013) 3244–3248.
[37] B. Long, Z. Ding, X. Wang, ChemSusChem 6 (2013) 2074–2078.
[38] I. Schlichting, J. Berendzen, K. Chu, A.M. Stock, S.A. Maves, D.E. Benson, R.M. Sweet, D. Ringe, G.A. Petsko, S.G. Sligar, Science 287 (2000) 1615–1622.
[39] W.M. Singh, D. Pegram, H. Duan, D. Kalita, P. Simone, G.L. Emmert, X. Zhao, Angew. Chem. Int. Ed. 51 (2012) 1653–1656.